ACS ES&T Water

pubs.acs.org/estwater

Article

Role of Nanoscale Morphology on the Efficiency of Solvent-Based Desalination Method

James S. Peerless, Alexey V. Gulyuk, Nina J. B. Milliken, Gyu Dong Kim, Elliot Reid, Jae Woo Lee, Dooil Kim, Zachary Hendren, Young Chul Choi, and Yaroslava G. Yingling*

Cite This: *ACS EST Water* 2023, 3, 400–409

Read Online

ACCESS | Metrics & More | Article Recommendations | Supporting Information

ABSTRACT: Brine desalination is important for minimizing the environmental impact of contaminated wastewater, yet current desalination techniques have high energy requirements. Solvent-based desalination (SBD) method, which is the process of extracting fresh water using an organic solvent, has existed for decades, yet has not reached competitive efficiencies. In this work, 10 organic solvents were tested for SBD efficacy via synergetic studies using bench-scale extraction experiments and molecular dynamics (MD) simulations. The SBD effectiveness was correlated to the computationally observed ability of the solvent to form one of the three morphologies in water: ordered, disordered, or partial nanoscale. We correlated that solvents that form ordered and disordered morphologies were not able to clean up the water. Solvents that were able to cause low salinity in water showed computationally observed partial nanoscale phase separation, where nanometer-scale aggregated solvent phases were able to effectively reject salt ions while capturing comparatively large amounts of water molecules. The formation of a partial nanoscale phase is likely driven by the solvent structure with bulky hydrocarbons adjacent to hydrophilic end groups. Our results make a step toward the rational design of solvents that may allow for efficient SBD and thus a low-cost source of fresh water.

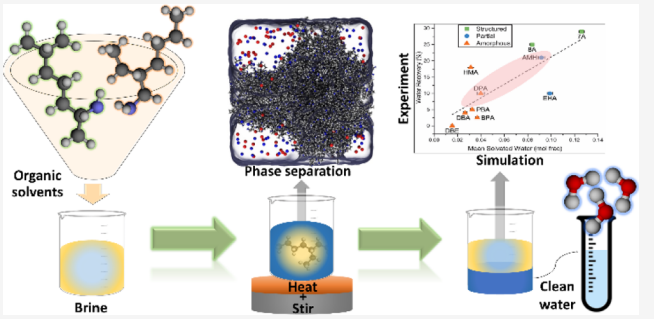

KEYWORDS: *solvent-based desalination, organic solvent, molecular dynamics simulation, temperature swing solvent extraction*

INTRODUCTION

Brine desalination is important. Clean water supply is among the greatest and most consequential challenges in the coming decades.[1] Thus, most current desalination technologies are focused on seawater and brackish water desalination. However, another source of water are hypersaline brines, which are water with very high levels of total dissolved solids (TDS >60,000 ppm). The hypersaline brines result from the concentrated wastewater after seawater desalination, landfill leachate, produced water from oil and gas activities, and other industrial activities. Because brines are usually discarded without treatment, they are a growing environmental concern.[2−5] The use of hypersaline brines for further water recovery is limited by both operational and economic hurdles, which prevent the use of predominant production-scale methods for desalination, such as multi-stage flash (MSF) and reverse osmosis (RO). RO technologies are the most energetically competitive, consuming less than one-fifth the energy required by state-of-the-art MSF methods on a per-volume basis.[6,7] However, RO processes require significant operating cost to extract freshwater from saline sources[7−9] and is not a viable technology for hypersaline brines. Hence, next-generation membranes with nanoscaled features[10−15] as well as non-membrane desalination methods[16−19] have been a subject of active research with the goal of increasing the efficiency of the desalination process.

The use of solvents to extract fresh water from saline sources has recently generated wide attention[20,21] because this approach avoids both the osmotic pressure issues that limit RO and the phase change energy needs of thermal desalination technologies[22−29] However, as early as 1960, Davison, Hood, and co-workers identified the prospects of using the variable solubility of water in organic solvents as a method of desalination of brine.[30,31] Because the solubility of a solvent can be governed by its intrinsic properties (like volatility) as well as by numerous external conditions, the use of solvents in aqueous solutions becomes a multi-stage process.[20] This solvent-based desalination (SBD) method (can be observed in Figure 1a and with more detail in Figure S1 of the Supporting Information), also frequently defined as solvent-driven aqueous separation (SDWE), solvent extraction

Received: September 23, 2022
Revised: January 4, 2023
Accepted: January 5, 2023
Published: January 25, 2023

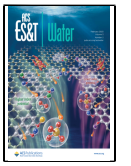

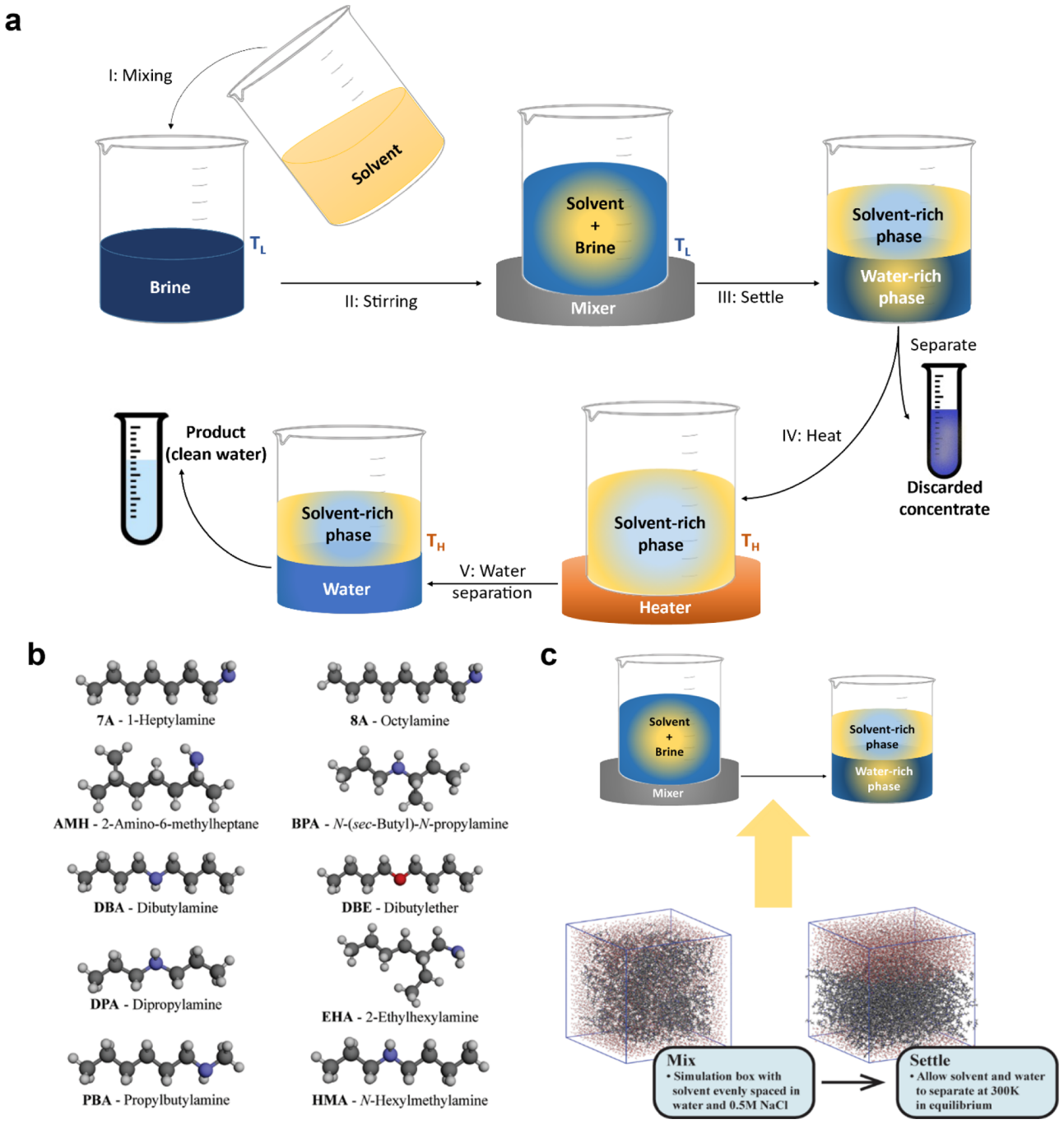

Figure 1. SBD method and experimental setup details: (a). Lab scale experiment procedure of SBD process. (b). Ten organic solvents and chemical naming abbreviations used in this study. (c). Graphical representation of simulation setup with representative simulation snapshots of DPA system. Snapshots and molecular structures colored by element H = white, red = O, gray = C, and blue = N.

desalination (SED), and temperature swing solvent extraction (TSSE), leverages the solvent's temperature-dependent solubility in water to extract pure water from a brine solution. Water and the solvent are first mixed and allowed to settle at an initial temperature (T_1). After settling, two phases are expected to form the following: solvent-rich phase and water-rich phase. The solvent-rich phase contains solvent and an amount of absorbed water with little-to-no salt, while the water-rich phase contains water and ions and becomes a more concentrated brine solution that can be discarded or run through the cycle again. The solvent-rich phase is then elevated to a higher temperature (T_2) at which the solubility of water in the solvent is lower which leads to precipitation of pure water out of solvent such that it can be recovered. The solvent can then be reused to avoid chemical waste.

According to various studies, this SBD method can be used not only for the desalination, but also for the removal and recovering of orthophosphates and their derivatives, as well as liquidous solutions like wastewater.[32−34] These solutions typically contain multiple pollutants, and their recovery requires sophisticated, and often tertiary multi-step approaches.[35] In this case, application of SBD may significantly advance the development of phosphate-removal approaches.[36] Particularly, adding solvent solutions as a pre-treatment

https://doi.org/10.1021/acsestwater.2c00473
ACS EST Water 2023, 3, 400−409

increases the efficiency of bioinspired phosphate removal.[37−39] Additionally, solvent-based methods can be utilized to recover phosphorus from other types of waste that may be presented in both soil and water.[40,41] Thus, utilization of solvents opens new paths to recovery the dangerous wastewater pollutants like heavy metals, nitrogen, hydrocarbons, and phosphorus.

After the initial work by Davison and Hood,[31] concerns over organic solvent leaching into the recovered water and the limits of feed water salinity reduced some interest in SBD as a viable seawater desalination approach.[22] More recently, interest has been renewed in SBD with the use of fatty acids, such as octanoic and decanoic acids, as the extraction solvent.[22−27] The use of a benign fatty acid eliminates the concern over solvent leaching, yet there is an apprehension over the overall efficiency of the process. The most recent estimates put the total energy density of a continuous SBD process with octanoic acid at less than 170 kWh/m^3 using conservative estimates of both thermal and electrical energy consumption.[27] For comparison, state-of-the-art thermal evaporator desalination processes have an energy density greater than 200 kWh/m^3,[42] suggesting that SBD can provide energy savings for high TDS brines. However, the energy intensity of SBD is largely dependent on the extraction solvent or solvent blend.[28] An ideal solvent would absorb a large amount of water while rejecting ions while also being insoluble in water to minimize solvent leftover in the fresh water supply. Moreover, if the temperatures at which water is absorbed (T_1) and precipitated (T_2) is close to ambient conditions, then the amount of energy required in the process can be greatly reduced.[27] Thus, small changes in the extraction solvent can have drastic effects on the overall viability of a SBD process. Yet to date, only a handful of solvents have been investigated for this application.[24]

This work aims to accelerate our understanding of atomic-scale behavior of the water-solvent-salt system by using a combination of experimental measurements and MD simulations that are used to quantify the efficacy of various organic solvents for use in solvent desalination. By taking this approach, we will improve our ability to assess and identify solvents that will provide superior desalination performance. All-atom molecular dynamics (MD) is a potentially powerful tool to efficiently screen solvent candidates for use in a SBD process and can reliably predict solvent behavior and properties.[43] MD has been previously used to calculate the relative solvation free energies of SBD solvents to identify decanoic and octanoic acid as viable candidates.[22,23,25] More broadly, MD has been applied to describe the nanoscale behavior of a variety of desalination membrane materials and ionic interactions.[12,15,44−49] In this work, a synergetic combination of all-atom MD simulations and SBD experimental measurements is used to quantify and explain the efficacy of 10 organic solvents that are mostly branched or with linear amines, with the exception of dibutyl ether (DBE), for use in the solvent desalination process (Figure 1b). These solvents were chosen as representative of a group of commercially available organic solvents with temperature-dependent water solubility that make them candidates as SBD extraction solvents. The efficacy of solvents at water extraction was measured both by bench-scale experiments as well as MD simulations. However, due to size and time scale limitation of MD simulations, we can only model the "Settle" process within the SBD cycle (Figure 1c). Thus, in this paper, we examine what occurs at the "Settle" stage and how it may be used to explain overall SBD efficiency as a function of solvent chemistry. Good agreement was observed between bench-scale experiments and simulation measurements.

METHODS

SBD Experiments. A solution of 0.5M NaCl was used as the synthetic brine for the bench scale experiments. Because the water solubility in the test solvent tends to decrease with the increase in temperature, the brine was mixed with the solvent at ambient temperature for water absorption and then the water was desorbed from the solvent by increasing the temperature .[50] The step-by-step experimental procedure is presented in Figure 1a. Here, (i) the known amount (20 mL) of brine is added to the solvent (20mL), (ii) the solvent and brine are mixed for 2 min by handshaking, (iii) the solvent-rich phase is separated from water-rich phase by gravity separation in 1 min, (iv) the solvent-rich phase liquid is heated at 80 °C for 2 h, and (v) water is desorbed from the solvent-rich phase liquid in 5 min and forms a layer at the bottom of the solvent-rich phase liquid. When the specific gravity of the solvent is larger than that of a brine, the solvent-rich phase locates under the water rich phase (iii) and the water layer forms on the surface of the solvent-rich phase. The fresh water was taken from the solvent-rich phase liquid and the volume is measured to determine percentage of recovery. Water quality parameters such as chemical oxygen demand (COD), pH, and Na and Cl concentrations are also measured.

The water recovery was calculated from dividing the product water volume by the feed water volume. The salt removal efficiency was calculated based on the concentration difference of the Cl^- ion between the feed water and product water. The pH was measured using litmus paper in small volume tests, and with a Hach pH electrode (Hach, HQ40D meter with PHC301 probe) for larger test volumes. The COD was measured using Hach TNT 822 kit with a spectrophotometer (Hach, DR6000), and the result is used to estimate the residual solvent in the product water. The concentration of Na and Cl in the brine and the product water was measured using ion chromatography (Thermo-Dionex, ICS3000). The Karl Fischer titrator (Mettler Toledo, V20 Volumetric KF Titrator) was used to analyze the water content in the solvent-rich phase liquid solution.

Computational Methods. MD simulations were performed to investigate the mixing and settling stage of the SBD process (see Figure 1). The simulation setup, along with representative visualizations is shown in Figure 1c. All simulations were performed with the AMBER 16 molecular dynamics package.[51] All solvent molecules underwent the same parameterization, equilibration, and simulation steps independently. The solvent structures were first drawn and energy minimized in Discovery Studio Visualizer.[52] Atomic partial charges were then calculated using the restrained electrostatic potential (RESP) method from ab initio calculations performed using the R.E.D. Server, Development.[53] All other force field parameters for the solvent were assigned using the general AMBER force field (GAFF), which is shown to be effective for room-temperature organic solvents.[54,55] Single molecules were then energy-minimized in AMBER using the steepest-descent method.

After the single molecule structure was energy minimized, 1000 solvent molecules were randomly placed in a box using the PACKMOL package.[56] The box volume was determined as twice the room-temperature volume of 1000 molecules of the solvent given that solvent's density, corresponding to

https://doi.org/10.1021/acsestwater.2c00473
ACS EST Water 2023, 3, 400−409

Table 1. Results from Bench-Top SBD Experiments[a]

solvent	water recovery (%)	Na rejection (%)	Cl rejection (%)	COD (mg/L)
1-heptylamine (7A)	29	−36[b]	−37[b]	6,414
octylamine (8A)	25	−32[b]	−30[b]	2,520
2-amino-6-methylheptane (AMH)	21	11	26	10,199
N-(*sec*-butyl)-*N*-propylamine (BPA)	2.5	99	99	43,000
dibutylamine (DBA)	4	100	99	14,100
dibutylether (DBE)	0	N/A	N/A	N/A
dipropylamine (DPA)	10	95	94	46,500
2-ethylhexylamine (EHA)	10	86	58	9,400
N-hexylmethylamine (HMA)	18	55	46	24,200
propylbutylamine (PBA)	5	99	98	53,550

[a]For DBE, there was no product water in the experiment, so either Cl or Na rejection was not measurable. [b]The negative values for 7 and 8 A mean the salt concentration in the product water was higher than that in the raw brine.

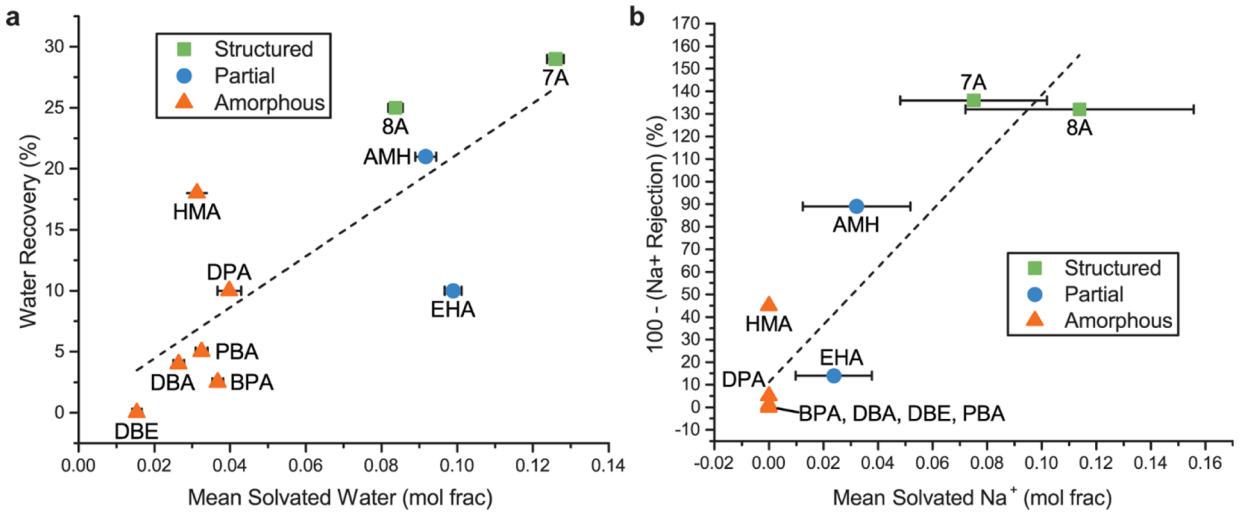

Figure 2. Correlation between MD simulation results (*x*-axis) and experiments (*y*-axis). Here, dashed line illustrates linear fit weighted for a round of experimental tests, and for averaged results of last 40 ns of MD simulations. The error bars indicate standard deviation of measurements taken in the last 40 ns of simulations. Symbols denote type of phase separation observed in simulation, discussed in more detail below. (a) Mean solvated water from MD simulations (*x*-axis) compared to experimentally measured water recovery (*y*-axis). (b) Mean solvated Na^+ ions from MD simulations (*x*-axis) compared to experimentally measured Na^+ rejection (*y*-axis).

approximately 80 Å × 80 Å x 80 Å in most cases. This box was then solvated with water with a 0.5 M (29,220 ppm) NaCl concentration using the AMBER tleap program. The TIP3P water model[57] and Li-Merz monovalent ion potentials[58] for Cl^- and Na^+ were chosen based on their compatibility with GAFF. This box containing salt water and solvent was then energy minimized and equilibrated for 500 ps with solvent molecules harmonically constrained under constant-temperature, constant-pressure (*NPT*) conditions at 300 K and 1 atm. This equilibration allows the salt water to reach a uniform temperature, while the solvent is harmonically constrained to disallow any phase separation. In this equilibration and all other non-vacuum simulations, periodic boundary conditions were applied to simulate an infinite volume with long range electrostatic interactions calculated via the particle mesh Ewald (PME) method. Temperature and pressure were maintained with the Langevin thermostat and the Berendsen barostat, respectively. Following this equilibration, the harmonic restraints are turned off and the system is run under *NPT* conditions at 300 K and 1 atm for 100 ns. Subsequent analysis of water and salt absorption, as well as solvent leftover, solvent order, and radial distribution functions were performed using a combination of CPPTRAJ,[59] the MDAnalysis Python package,[60] and in-house analysis scripts as described in previous publications[61,62] and the Results section below. Simulation snapshots are visualized with VMD.[63]

RESULTS AND DISCUSSION

Experimental results from the bench-scale SBD experiments are summarized in Table 1 below. There are four primary figures of merit: water recovery, Na rejection, Cl rejection, and COD in the recovered water, which quantifies the amount of solvent that has entered the water phase and remains present in the fresh water after recovery. We note that some solvents, such as AMH, EHA, and HMA, exhibited very different rejection efficiencies of Na+ versus Cl-ions. This can be explained by the difference of solvation free energies between Na+ and Cl-in water and solvent.[23] For example, the solvation free energies of Na+ in decanoic acid and in water were −72.44 and −90.10 kcal/mol, respectively, while those of Cl- were −64.70 and −75.40 kcal/mol, respectively. This indicates that an uneven rejection of Na+ and Cl- may occur due to their differences in solvation free energies in solvents and water.

In experiments, the solvent leftover (as quantified by COD in Table 1) is an important characteristic. For any SBD cycle, it is critical that the directional solvent is not present in the

https://doi.org/10.1021/acsestwater.2c00473
ACS EST Water 2023, 3, 400−409

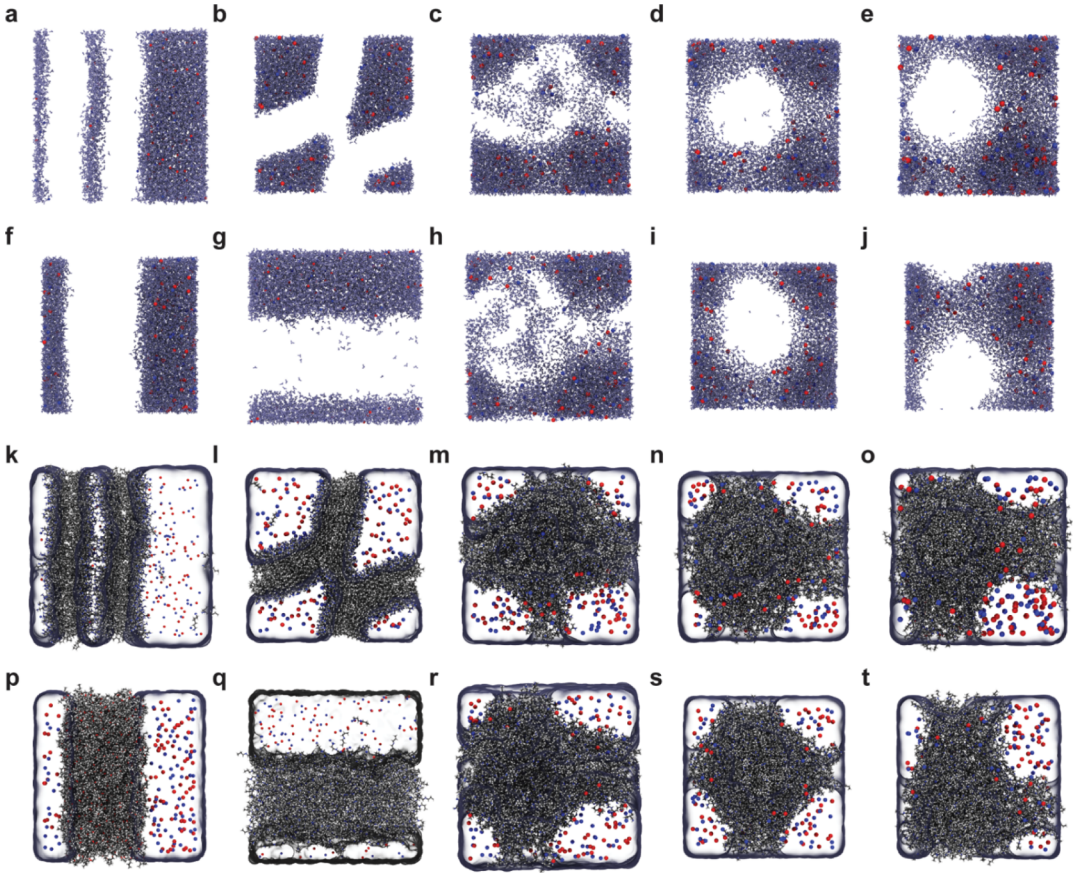

Figure 3. Visualizations of phase separation in water-solvent-ion systems at the end of the 100 ns production run. (a–j) Only water (light blue) and ions (Cl^- = red spheres and Na^+ = blue spheres) shown for clarity (solvent not shown). (k–t) Only solvent (licorice representation; H = white, C = gray, N = blue, and O = red) and ions (Cl^- = red spheres and Na^+ = blue spheres) shown for clarity (water depicted as a transparent surface). Solvents in alphabetical order: (a,k) 7A, (b,l) 8A, (c,m) AMH, (d,n) BPA, (e,o) DBA, (f,p) DBE, (g,q) DPA, (h,r) EHA, (i,s) HMA, and (j,t) PBA.

recovered water above harmful levels. The allowable limit of solvent in the recovered water is very diverse, depending on the toxicity of the extraction solvent. Nonetheless, it should be noted that most of the directional solvents investigated in this study are potentially hazardous and thus it would be necessary to ensure that little to no directional solvent remains in the recovered water. Although the remaining solvent in the recovered water may be estimated by the amount of hydrated solvent (as measured from simulation), the limited number of solvent molecules simulated results in only one or two solvent molecules escaping to the water-rich phase (see Supporting Information, Figure S2b). Consequently, there is a large amount of statistical noise in the hydrated solvent simulation data. The resulting limited statistical significance does not allow for effective comparison of solvent leftover between solvents and is thus omitted in the discussion of the simulation results.

Hence, the primary indicators of solvent efficacy from the simulations are the amount of water and ionic species that have entered the solvent phase. These values correspond to the water recovery and the inverse of salt rejection, respectively, as measured from bench-scale experiments. To calculate this, the frames of the 100ns trajectories were analyzed using a script to calculate the fraction of (a) solvated water, (b) solvated Na^+ ions, (c) solvated Cl^- ions, and (d) in the aqueous phase (indicative of solvent leftover) at snapshots every 2 ns. Solvated ions and water molecules are defined as those with greater than 15 solvent atoms in the first solvation shell (within 4 Å) of the ion or molecule. Similarly, hydrated solvent molecules (analogous to solvent leftover) are those containing greater than 30 water molecules in the first solvation shell (within 4 Å) of the solvent molecule. We defined the solvation shell distances, number of atoms in solvated, and hydrated phase to be the same for all solvents and system configurations across the simulations performed. These number can be derived computationally[64] and were determined them from the radial distribution function data of our MD production runs.

Results from all calculated values indicate that all runs reached a steady state in terms of species solvation after approximately 60 ns (see Supporting Information, Figure S2). All solvated water measurements made in the last 40 ns of MD simulations are averaged and shown in Figure 2a compared with experimentally measured water recovery values. Large error bars (e.g., in case of 7A and 8A in Figure 2b) indicate the variations in amount of solvated Na + that were detected across the simulation timeframe (last 40 ns). Comparison of the values calculated from simulation and those calculated from experiment show a strong positive correlation (Pearson's r = 0.784), with the calculated R^2 value equal to 0.602. Similarly, the amount of solvated Na^+ ions are very strongly correlated (Pearson's r = 0.903) with R^2 = 0.798, and with the inverse of rejected Na^+ as measured by experiment, as shown in Figure 2b. As can be seen, EHA and HMA show large deviations from the linear fit, possibly because water recovery and solvated Na^+ are both under-estimated by simulation. For

https://doi.org/10.1021/acsestwater.2c00473
ACS EST Water 2023, 3, 400–409

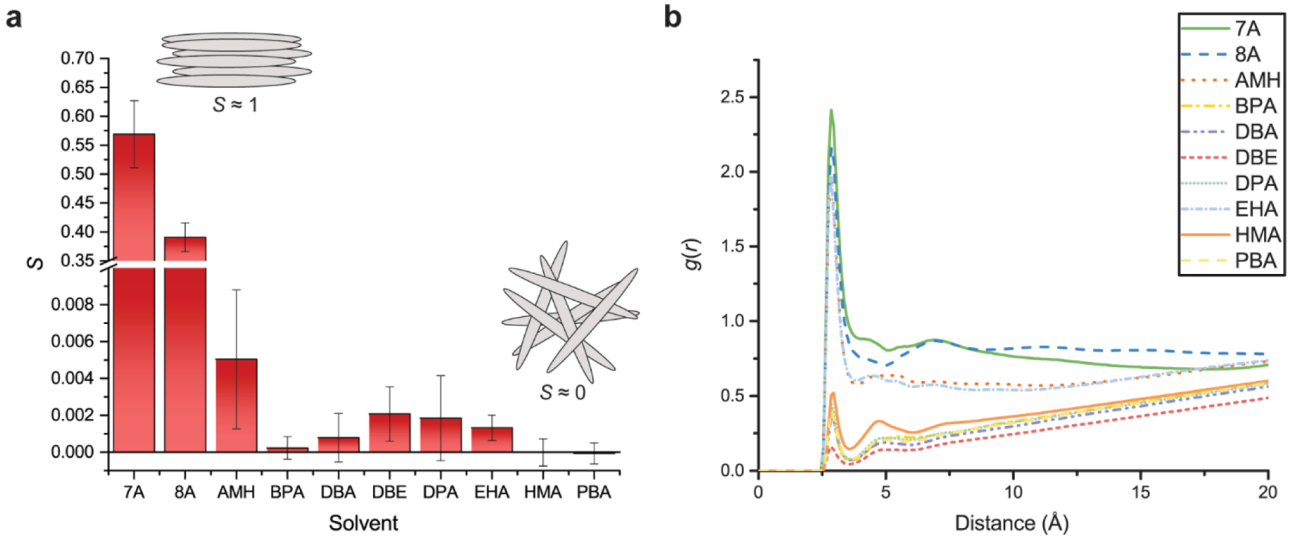

Figure 4. Solvent-rich phase structure data. (a) Solvent order parameter (S) calculated from simulations for each solvent. Here the error bars indicate standard deviation of measurements taken in the last 40 ns of MD simulations. Graphical insets: illustration of ordered and disordered system. (b) Radial distribution functions [$g(r)$] of hydrophilic solvent atom (N or O) to water oxygen atoms calculated over the last 40 ns of simulation.

additional information regarding Cl-ion solvation, one can refer to the Section S2 of Supporting Information

While the numerical data discussed above provides corroborative data between simulation and experiment, the ability for simulations to be visualized can provide even further insights into the nanoscale phenomena occurring at the early stages of phase separation. For example, the snapshots of the water and ions in each system at the end of 100 ns are visualized in Figure 3a–j. From these images, one can clearly identify different levels of phase separation. Although stable amounts of solvated water and hydrated solvent were calculated for all systems at the time of these snapshots, both AMH (Figure 3c) and EHA (Figure 3h) do not appear to be fully phase separated in the general sense of the term. There appear to be small (nanometer scale) metastable regions of water in which water molecules more freely move in and out with relatively few ionic species remaining (this can be seen more clearly in video form. See Movie S2 in Supporting Information < Supporting Information/Video Link > for an animation of EHA during the stable period of the 100ns simulation.). Hence, the AMH and EHA systems are considered partially nanoscale phase separated.

As the structure of water-rich phases diverge based on the solvent species shown in Figure 3a–j, so too do the behavior of the solvent-rich phases. Figure 3k–t shows snapshots of the identical systems in Figure 3a–j, only the solvent is visualized, and the water is represented as a transparent surface. In this case, one can quickly notice a qualitative difference between the solvent-rich phase depicted for 7A (Figure 3k) and 8A (Figure 3l) and the other solvent phases. As one might expect based on the structure of these two solvents, the molecules appear to be self-assembling into bilayers with the hydrophilic nitrogen creating an interface with the water-rich phase and the hydrophobic hydrocarbon tails pointing toward each other.

To quantify the effect depicted in Figure 3k,l, the nematic order parameter, S,[65] was calculated from the last 40ns of each simulation. This parameter, typically applied to liquid crystals,[66] is defined in eq 1 as follows:

$$S = \left\langle \frac{3\cos^2\theta - 1}{2} \right\rangle \quad (1)$$

where θ is the angle between two linear polymers and the angle brackets denote averaging over time and space. This parameter provides a basic summary of the alignment of linear molecules in a dynamic system: $S = 1$ indicates a perfectly aligned sample, while $S = 0$ is a completely random alignment of molecules (See Figure 4a, graphical insets). For these systems, the solvents were reduced to vectors along the longest continuous chain of the solvent molecule with the vector terminating at the end of the carbon chain. This was done for calculation of θ between all solvent molecule pairs at 10ns intervals in the last 40 ns of each simulation. The resulting values of S for each solvent are shown in Figure 4a. The results definitively show that 7A and 8A undergo significant structured self-assembly, while the solvent-rich phase of all other solvents can be considered amorphous. Hence, here we define systems of 7A and 8A as undergoing ordered phase separation.

The simulated solvents can thus be categorized into three methods of phase separation: structured phase separation (7A, 8A), partial nanoscale phase separation (AMH, EHA), and amorphous phase separation (BPA, DBE, DPA, HMA, and PBA). The amphiphilic structure of 7A and 8A serves as a clear indicator of the likelihood for structured self-assembly, yet this feature is not particularly useful for SBD applications. As indicated by both experiment and simulation, these solvents are successful at recovering large percentage of water but are weak at rejecting salt. This may be explained, as was observed in simulation, by the formation of bilayers surrounding large phases of water that also contain ionic species at the original brine concentration (Figure 3k,l). In other words, the surfactant-like structure of these solvents can successfully capture water phases but does not selectively reduce the amount of ionic species.

In contrast, the solvents that undergo partial nanoscale phase separation during MD simulations, AMH and EHA, exhibit behavior that was not expected based on the solvent structure alone. Although EHA showed moderate water

https://doi.org/10.1021/acsestwater.2c00473
ACS EST Water 2023, 3, 400–409

recovery and salt rejection experimentally, the existence of nanoscale phases of pure water observed during our simulations indicate a very interesting morphological feature. The presented nanoscale phases, if properly leveraged, could absorb much larger quantities of water (compared to amorphous phase-separating solvents) while still rejecting salt. Even though the carried-out MD simulations do not allow us to provide exact environmental parameters (like optimal solvent structure, temperature, stirring mode, mixing speed, or related parameters) to maximize the presence of such phases, this finding can serve as a starting point for further investigations, especially if being conjugated with other recently available studies.[67,68] It is possible, that these phases would no longer exist after hours of equilibrium conditions, yet the persistence of such phases over the simulation time and the correlation of experimental and simulation measurements do suggest that such phases are at least metastable and have a macroscopic effect on desalination measurements after settling.

The phenomena of partial nanoscale phase separation were not predicted a priori. However, examining the structure of EHA and AMH suggests that partial nanoscale phase separation is somewhat analogous to what was observed for the structured phase-separating solvents (7A and 8A). Both EHA and AMH contain hydrophilic nitrogen at the terminus of the molecule. However, unlike the surfactant-like 7A and 8A, these molecules have additional bulky groups adjacent to the hydrophilic atom—an ethyl group in the case of EHA and a methyl group for AMH. It is hypothesized that the availability of hydrophilic nitrogen encourages a higher concentration of these groups at the solvent−water interface, but the bulkiness of adjacent groups discourages the structured ordering exhibited by 7A and 8A. A comparison of these solvent−water interfaces can be seen in Figure 3a,b and explained as follows: for amorphous phase separations, the hydrophilic atom is restricted from assembling at the organic surface, whereas in the case of EHA and AMH, the solvent molecules can orient such that a higher concentration of nitrogen can be maintained at the interface.

The ability for the amphiphilic groups to arrange at the surface for EHA and AMH is further supported by the radial distribution function (RDF) data shown in Figure 4b. The RDFs were calculated between the hydrophilic atom on the solvent molecules (N, or O for DBE) to water oxygen atoms in the last 40ns of each simulation. This value gives the probability of finding a water molecule at a particular distance from the hydrophilic solvent atom relative to the bulk water density. In all the amorphous phase separation cases (BPA, DBE, DPA, HMA, and PBA), the RDF value starts below one and slopes toward one at a distance of 40 Å (approximately half the simulation box length). This indicates that one is less likely to find a water molecule near the hydrophilic atom, rather than if water was uniformly distributed throughout the box, as one would expect from a strongly phase separated system.

Conversely, the structured phase separated systems (7A, 8A) show a large distinct peak at a distance of approximately 4Å. This indicates a high probability of finding a water molecule directly next to the hydrophilic atom, an expected result given the morphology observed in these systems (see Figure 3k,l). The systems that undergo partial nanoscale phase separation (EHA and AMH, respectively), however, are somewhat in between the two extremes. While there is a strong first peak, as seen in the structured solvents, the RDF is significantly lower at intermediate distances. This shows that water is likely to be organized near these solvent atoms, yet two or three solvation shells out there is a less-defined water phase. Hence, while the hydrophilic solvent atoms organize at the surface, the branched nature of EHA and AMH disallows the strong self-assembly observed in 7A and 8A.

CONCLUSIONS

A synergetic studies involving bench-scale extraction experiments and all-atom MD simulations were performed on 10 organic solvents as candidates for SBD. Simulation results correlate strongly with water recovery and salt rejection measurements from the experiment. The atomistic scale of simulation allows for a clear investigation of the phase separation of solvent and water and thus provides insights into the mechanisms of water absorption and salt rejection. Three modes of phase separation were identified: structured, amorphous, and partial nanoscale phase separation. While the formation of structured or amorphous phase separation was not favorable for efficient salt extraction, the partial nanoscale phase separation arises particularly in nanoscale regions of water with little to no salt inclusion, which may be useful for efficient SBD. The formation of a partial nanoscale separated phase is likely driven by the structure of the solvent, having bulky hydrocarbons adjacent to hydrophilic end groups.

The identification of this partial nanoscale phase separation phenomena may greatly increase the amount of water that may be recovered from each individual SBD cycle. The solvents investigated here may not yet be as effective at salt rejection as would ultimately be desired. However, identification of molecular structural features in our study may lead to the rational design of extraction solvents that could efficiently reject salt while absorbing large quantities of water at room temperature. Moreover, solvents that were observed to undergo amorphous phase separation all exhibited excellent salt rejection and various levels of water absorption. Further identifying molecular structures that allow for higher amounts of absorbed water in amorphous structures while maintaining superlative salt rejection is also a promising avenue for rational solvent design. More experiments could be fruitful in determining a solvent that meets all the requirements of an ideal extraction solvent provided the knowledge that nanoscale effects can be leveraged for efficient water capture. This, in turn, could go a long way in making SBD not only an energetically viable alternative to RO and MSF technologies but also a promising approach in the utilization of solvents for recovery of the wastewater pollutants like heavy metals, nitrogen, hydrocarbons, and phosphorus.

ASSOCIATED CONTENT

Supporting Information

The Supporting Information is available free of charge at https://pubs.acs.org/doi/10.1021/acsestwater.2c00473.

Diagram of the SBD process to extract water from a brine solution using an organic solvent with temperature-dependent water solubility; details from MD simulations; details of the available experimental data; measurements of solvated water, hydrated solvent (solvent leftover), solvated Na+, and solvated Cl from last 100 ns of MD simulations shown over time phase; and separation dynamics representative snapshots (PDF)

https://doi.org/10.1021/acsestwater.2c00473
ACS EST Water 2023, 3, 400−409

Phase separation dynamics representing ordered phase separation, disordered phase separation, and partial nanoscale phase separation (ZIP)

Disordered phase separation dynamics (ZIP)

AUTHOR INFORMATION

Corresponding Author

Yaroslava G. Yingling − *Department of Materials Science and Engineering, North Carolina State University, Raleigh, North Carolina 27695, United States;* orcid.org/0000-0002-8557-9992; Email: yara_yingling@ncsu.edu

Authors

James S. Peerless − *Department of Materials Science and Engineering, North Carolina State University, Raleigh, North Carolina 27695, United States;* orcid.org/0000-0002-8973-5577

Alexey V. Gulyuk − *Department of Materials Science and Engineering, North Carolina State University, Raleigh, North Carolina 27695, United States;* orcid.org/0000-0002-9924-8713

Nina J. B. Milliken − *Department of Materials Science and Engineering, North Carolina State University, Raleigh, North Carolina 27695, United States*

Gyu Dong Kim − *Center for Technology Advancement & Commercialization, RTI International, Research Triangle Park, North Carolina 27709, United States;* orcid.org/0000-0002-4233-9729

Elliot Reid − *School of Civil and Environmental Engineering, Georgia Institute of Technology, Atlanta, Georgia 30332, United States*

Jae Woo Lee − *Department of Environmental Engineering, Korea University, Sejong 339-700, Korea;* orcid.org/0000-0002-4376-476X

Dooil Kim − *Department of Civil and Environmental Engineering, Dankook University, Yongin, Gyeonggi-do 16890, Korea*

Zachary Hendren − *A.R. Smith Department of Chemistry & Fermentation Sciences, Appalachian State University, Boone, North Carolina 28608, United States*

Young Chul Choi − *Research & Development Center, Saudi Aramco, Dhahran 31311, Saudi Arabia*

Complete contact information is available at: https://pubs.acs.org/10.1021/acsestwater.2c00473

Author Contributions

CRediT: **James Samuel Peerless** conceptualization (equal), data curation (supporting), formal analysis (lead), investigation (lead), methodology (supporting), visualization (lead), writing-original draft (lead); **Alexey V. Gulyuk** data curation (lead), visualization (supporting), writing-review & editing (supporting); **Nina J. B. Milliken** investigation (supporting); **Gyu Dong Kim** formal analysis (supporting), investigation (lead), methodology (lead), validation (lead), writing-review & editing (supporting); **Elliot M. Reid** formal analysis (supporting), investigation (supporting); **Young Chul Choi** conceptualization (lead), funding acquisition (lead), investigation (supporting), methodology (supporting), project administration (supporting), supervision (supporting), writing-review & editing (supporting); **Yaroslava G Yingling** conceptualization (lead), data curation (supporting), funding acquisition (lead), methodology (lead), project administration (lead), resources (lead), supervision (lead), writing-review & editing (lead).

Notes

The authors declare no competing financial interest.

Disclaimer. This paper was prepared as an account of work sponsored by an agency of the United States Government. Neither the United States Government nor any agency thereof, nor any of their employees, makes any warranty, express or implied, or assumes any legal liability or responsibility for the accuracy, completeness, or usefulness of any information, apparatus, product, or process disclosed, or represents that its use would not infringe privately owned rights. Reference herein to any specific commercial product, process, or service by trade name, trademark, manufacturer, or otherwise does not necessarily constitute or imply its endorsement, recommendation, or favoring by the United States Government or any agency thereof. The views and opinions of authors expressed herein do not necessarily state or reflect those of the United States Government or any agency thereof.

This paper contains Supporting Information section containing additional background materials on SBD process, detailed description of MD simulation systems, additional information on performance of organic solvents on salts capture and water recovery (experimental and simulation data), as well as animations and movies representing the dynamics and phase separation stages of the desalination process. This material is available free of charge via the internet at http://pubs.acs.org.

ACKNOWLEDGMENTS

The authors gratefully acknowledge support for this work through the Game-Changing Research Incentive Program (GRIP), a research seed-funding initiative coordinated and supported by the NC State Office of Research and Innovation (ORI), RTI International, and the Kenan Institute for Engineering, Science and Technology and by the Science and Technologies for Phosphorus Sustainability (STEPS) Center, a National Science Foundation Science and Technology Center (CBET-2019435). The authors also acknowledge additional funding provided by the National Science Foundation Research Traineeship on Data-Enabled Science and Engineering of Atomic Structures (DGE-1633587), from the Department of Energy's National Energy Technology Laboratory under cooperative agreement (DE-FE0024074), and from the Korea Agency for Infrastructure Technology Advancement (KAIA) grant funded by the Ministry of Land, Infrastructure and Transport (Grant 18CTAP-C128926-02).

REFERENCES

(1) Eliasson, J. The rising pressure of global water shortages. *Nature* **2014**, *517*, 6.

(2) Gregory, K. B.; Vidic, R. D.; Dzombak, D. A. Water management challenges associated with the production of shale gas by hydraulic fracturing. *Elements* **2011**, *7*, 181−186.

(3) Pramanik, B. K.; Shu, L.; Jegatheesan, V. A review of the management and treatment of brine solutions. *Environmental science: water research & technology* **2017**, *3*, 625−658.

(4) Tong, T.; Elimelech, M. The global rise of zero liquid discharge for wastewater management: drivers, technologies, and future directions. *Environmental science & technology* **2016**, *50*, 6846−6855.

(5) Renou, S.; Givaudan, J.; Poulain, S.; Dirassouyan, F.; Moulin, P. Landfill leachate treatment: Review and opportunity. *Journal of hazardous materials* **2008**, *150*, 468−493.

(6) Elimelech, M.; Phillip, W. A. The Future of Seawater Desalination: Energy, Technology, and the Environment. *Science* **2011**, *333*, 712−717.
(7) Rao, P.; Morrow, W. R.; Aghajanzadeh, A.; Sheaffer, P.; Dollinger, C.; Brueske, S.; Cresko, J. Energy considerations associated with increased adoption of seawater desalination in the United States. *Desalination* **2018**, *445*, 213−224.
(8) Karabelas, A. J.; Koutsou, C. P.; Kostoglou, M.; Sioutopoulos, D. C. Analysis of specific energy consumption in reverse osmosis desalination processes. *Desalination* **2018**, *431*, 15−21.
(9) Service, R. F. Desalination Freshens Up. *Science* **2006**, *313*, 1088−1090.
(10) Yang, Z.; Ma, X.-H.; Tang, C. Y. Recent development of novel membranes for desalination. *Desalination* **2018**, *434*, 37−59.
(11) Wang, Z.; Wang, Z.; Lin, S.; Jin, H.; Gao, S.; Zhu, Y.; Jin, J. Nanoparticle-templated nanofiltration membranes for ultrahigh performance desalination. *Nat. Commun.* **2018**, *9*, 2004.
(12) Jamali, S. H.; Vlugt, T. J. H.; Lin, L.-C. Atomistic Understanding of Zeolite Nanosheets for Water Desalination. *The Journal of Physical Chemistry C* **2017**, *121*, 11273−11280.
(13) Mauter, M. S.; Zucker, I.; Perreault, F. o.; Werber, J. R.; Kim, J.-H.; Elimelech, M. The role of nanotechnology in tackling global water challenges. *Nature Sustainability* **2018**, *1*, 166−175.
(14) Lee, J.; Wang, R.; Bae, T.-H. High-performance reverse osmosis membranes fabricated on highly porous microstructured supports. *Desalination* **2018**, *436*, 48−55.
(15) Sun, L.; He, X.; Lu, J. Super square carbon nanotube network: a new promising water desalination membrane. *npj Computational Materials* **2016**, *2*, 16004.
(16) Chen, H.-C.; Chen, Y.-R.; Yang, K.-H.; Yang, C.-P.; Tung, K.-L.; Lee, M.-J.; Shih, J.-H.; Liu, Y.-C. Effective reduction of water molecules' interaction for efficient water evaporation in desalination. *Desalination* **2018**, *436*, 91−97.
(17) Feng, C.; Chen, Y.-A.; Yu, C.-P.; Hou, C.-H. Highly porous activated carbon with multi-channeled structure derived from loofa sponge as a capacitive electrode material for the deionization of brackish water. *Chemosphere* **2018**, *208*, 285−293.
(18) Desai, D.; Beh, E. S.; Sahu, S.; Vedharathinam, V.; van Overmeere, Q.; de Lannoy, C. F.; Jose, A. P.; Völkel, A. R.; Rivest, J. B. Electrochemical Desalination of Seawater and Hypersaline Brines with Coupled Electricity Storage. *ACS Energy Letters* **2018**, *3*, 375−379.
(19) Boo, C.; Winton, R. K.; Conway, K. M.; Yip, N. Y. Membrane-less and non-evaporative desalination of hypersaline brines by temperature swing solvent extraction. *Environmental Science & Technology Letters* **2019**, *6*, 359−364.
(20) Foo, Z. H.; Stetson, C.; Dach, E.; Deshmukh, A.; Lee, H.; Menon, A. K.; Prasher, R.; Yip, N. Y.; Lienhard, J. H.; Wilson, A. D. Solvent-driven aqueous separations for hypersaline brine concentration and resource recovery. *Trends in Chemistry* **2022**, *4*, 1078−1093.
(21) Schuur, B.; Brouwer, T.; Sprakel, L. M. J. Recent Developments in Solvent-Based Fluid Separations. *Annual Review of Chemical and Biomolecular Engineering* **2021**, *12*, 573−591.
(22) Bajpayee, A.; Luo, T.; Muto, A.; Chen, G. Very low temperature membrane-free desalination by directional solvent extraction. *Energy Environ. Sci.* **2011**, *4*, 1672.
(23) Luo, T.; Bajpayee, A.; Chen, G. Directional solvent for membrane-free water desalination—A molecular level study. *J. Appl. Phys.* **2011**, *110*, 054905.
(24) Bajpayee, A.*Directional Solvent Extraction Desalination*; Massachusetts Institute of Technology, 2012.
(25) Rish, D.; Luo, S.; Kurtz, B.; Luo, T. Exceptional ion rejection ability of directional solvent for non-membrane desalination. *Appl. Phys. Lett.* **2014**, *104*, 024102.
(26) Sanap, D. B.; Kadam, K. D.; Narayan, M.; Kasthurirangan, S.; Nemade, P. R.; Dalvi, V. H. Analysis of saline water desalination by directed solvent extraction using octanoic acid. *Desalination* **2015**, *357*, 150−162.
(27) Alotaibi, S.; Ibrahim, O. M.; Luo, S.; Luo, T. Modeling of a continuous water desalination process using directional solvent extraction. *Desalination* **2017**, *420*, 114−124.
(28) Chaoui, I.; Abderafi, S.; Vaudreuil, S.; Bounahmidi, T. Water desalination by forward osmosis: draw solutes and recovery methods−review. *Environmental Technology Reviews* **2019**, *8*, 25−46.
(29) Choi, O. K.; Seo, J. H.; Kim, G. S.; Hendren, Z.; Kim, G. D.; Kim, D.; Lee, J. W. Non-membrane solvent extraction desalination (SED) technology using solubility-switchable amine. *J. Hazard. Mater.* **2021**, *403*, 123636.
(30) Davidson, R. R.; Smith, W. H.; Hood, D. W. Structure and Amine-Water Solubility in Desalination by Solvent Extraction. *Journal of Chemical & Engineering Data* **1960**, *5*, 420−423.
(31) Davison, R. R.; Hood, D. W. Thermodynamic Cycles for Recovery of Water by Solvent Extraction. *Industrial & Engineering Chemistry Process Design and Development* **1964**, *3*, 399−404.
(32) Mwabonje, O. N.; Jiang, J.-Q. A trial of using solvent extraction for phosphorus recovery. *Journal of Water Resource and Protection* **2010**, *02*, 830.
(33) Ilyas, S.; Srivastava, R. R.; Kim, H. Liquid-liquid extraction of phosphorus from sulfuric acid solution using benzyl dimethyl amine. *International Journal of Minerals, Metallurgy and Materials* **2021**, *28*, 367−372.
(34) Vandegrift, G. F.; Horwitz, E. P. Interfacial activity of liquid-liquid extraction reagents—I: Dialkyl phosphorous based acids. *Journal of Inorganic and Nuclear Chemistry* **1980**, *42*, 119−125.
(35) Mat Aron, N. S.; Khoo, K. S.; Chew, K. W.; Veeramuthu, A.; Chang, J.-S.; Show, P. L. Microalgae cultivation in wastewater and potential processing strategies using solvent and membrane separation technologies. *Journal of Water Process Engineering* **2021**, *39*, 101701.
(36) Jones, J. L.; Yingling, Y. G.; Reaney, I. M.; Westerhoff, P. Materials matter in phosphorus sustainability. *MRS Bull.* **2020**, *45*, 7−10.
(37) Chew, K. W.; Chia, S. R.; Krishnamoorthy, R.; Tao, Y.; Chu, D.-T.; Show, P. L. Liquid biphasic flotation for the purification of C-phycocyanin from Spirulina platensis microalga. *Bioresour. Technol.* **2019**, *288*, 121519.
(38) Leong, H. Y.; Ooi, C. W.; Law, C. L.; Julkifle, A. L.; Ling, T. C.; Show, P. L. Application of liquid biphasic flotation for betacyanins extraction from peel and flesh of Hylocereus polyrhizus and antioxidant activity evaluation. *Sep. Purif. Technol.* **2018**, *201*, 156−166.
(39) Sankaran, R.; Show, P. L.; Cheng, Y.-S.; Tao, Y.; Ao, X.; Nguyen, T. D. P.; Van Quyen, D. Integration Process for Protein Extraction from Microalgae Using Liquid Biphasic Electric Flotation (LBEF) System. *Mol. Biotechnol.* **2018**, *60*, 749−761.
(40) Ügdüler, S.; Van Geem, K. M.; Roosen, M.; Delbeke, E. I. P.; De Meester, S. Challenges and opportunities of solvent-based additive extraction methods for plastic recycling. *Waste Management* **2020**, *104*, 148−182.
(41) Anderson, L. Y. E. C. W.-T.; Yu, E.; Chen, W.-T. Chemical Recycling of Mixed Plastics in Electronic Waste Using Solvent-Based Processing. *Processes* **2022**, *10* (1), 66.
(42) Kaplan, R.; Mamrosh, D.; Salih, H. H.; Dastgheib, S. A. Assessment of desalination technologies for treatment of a highly saline brine from a potential CO2 storage site. *Desalination* **2017**, *404*, 87−101.
(43) Wang, J.; Hou, T. Application of Molecular Dynamics Simulations in Molecular Property Prediction. 1. Density and Heat of Vaporization. *J. Chem. Theory Comput.* **2011**, *7*, 2151−2165.
(44) Kolev, V.; Freger, V. Molecular Dynamics Investigation of Ion Sorption and Permeation in Desalination Membranes. *The Journal of Physical Chemistry B* **2015**, *119*, 14168−14179.
(45) Qiu, Y.; Schwegler, B. R.; Wang, L.-P. Polarizable Molecular Simulations Reveal How Silicon-Containing Functional Groups Govern the Desalination Mechanism in Nanoporous Graphene. *J. Chem. Theory Comput.* **2018**, *14*, 4279−4290.
(46) Zhang, N.; Chen, S.; Yang, B.; Huo, J.; Zhang, X.; Bao, J.; Ruan, X.; He, G. Effect of Hydrogen-Bonding Interaction on the

Arrangement and Dynamics of Water Confined in a Polyamide Membrane: A Molecular Dynamics Simulation. *The Journal of Physical Chemistry B* **2018**, *122*, 4719−4728.
(47) Barbosa, G. D.; Liu, X.; Bara, J. E.; Weinman, S. T.; Turner, C. H. High-salinity brine desalination with amine-based temperature swing solvent extraction: A molecular dynamics study. *J. Mol. Liq.* **2021**, *341*, 117359.
(48) Sappidi, P. Molecular simulation of separation of gadolinium ions from aqueous waste using directional solvent extraction. *J. Mol. Liq.* **2021**, *341*, 117330.
(49) Kim, M.; Choi, O. K.; Cho, Y.; Lee, J. W.; Cho, A. E. Elucidation of the desalination mechanism of solvent extraction method through molecular modeling studies. *Desalination* **2020**, *496*, 114704.
(50) Choi, O. k.; Kim, M.; Cho, A. E.; Choi, Y. C.; Kim, G. D.; Kim, D.; Lee, J. Fates of water and salts in non-aqueous solvents for directional solvent extraction desalination: Effects of chemical structures of the solvents. *Membrane Water Treatment* **2019**, *10*, 207−212.
(51) Case, D. A. R. M. B.; Cerutti, D. S.; Cheatham, T. E., III; Darden, T. A.; Duke, R. E.; Giese, T. J.; Gohlke, H.; Goetz, A. W. N. H.; Izadi, S.; Janowski, P.; Kaus, J.; Kovalenko, A.; Lee, T. S.; LeGrand, S.; Li, P. C.; Lin, T. L.; Luo, R.; Madej, B.; Mermelstein, D.; Merz, K. M.; Monard, G.; Nguyen, H.; Nguyen, H. T. I.; Omelyan, A. O.; Roe, D. R.; Roitberg, A.; Sagui, C.; Simmerling, C. L.; Botello-Smith, W. M.; Swails, J.; Walker, R. C. J. W.; Wolf, R. M.; Wu, X.; Xiao, L.; Kollman, P. A.*AMBER 2016*; University of California: San Francisco, 2016.
(52) Accelrys Software, I.. *Discovery Studio Visualizer*: San Diego, 2013; Vol. *4.0*.
(53) Vanquelef, E.; Simon, S.; Marquant, G.; Garcia, E.; Klimerak, G.; Delepine, J. C.; Cieplak, P.; Dupradeau, F.-Y. R. E. D. Server: a web service for deriving RESP and ESP charges and building force field libraries for new molecules and molecular fragments. *Nucleic Acids Res.* **2011**, *39*, W511−W517.
(54) Wang, J.; Wolf, R. M.; Caldwell, J. W.; Kollman, P. A.; Case, D. A. Development and testing of a general amber force field. *J. Comput. Chem.* **2004**, *25*, 1157−1174.
(55) Peerless, J. S.; Kwansa, A. L.; Hawkins, B. S.; Smith, R. C.; Yingling, Y. G. Uncertainty Quantification and Sensitivity Analysis of Partial Charges on Macroscopic Solvent Properties in Molecular Dynamics Simulations with a Machine Learning Model. *J. Chem. Inf. Model.* **2021**, *61*, 1745−1761.
(56) Martínez, L.; Andrade, R.; Birgin, E. G.; Martínez, J. M. PACKMOL: A Package for Building Initial Configurations for Molecular Dynamics Simulations. *J. Comput. Chem.* **2009**, *30*, 2157−2164.
(57) Jorgensen, W. L.; Chandrasekhar, J.; Madura, J. D.; Impey, R. W.; Klein, M. L. Comparison of simple potential functions for simulating liquid water. *J. Chem. Phys.* **1983**, *79*, 926−935.
(58) Li, P.; Song, L. F.; Merz, K. M. Systematic Parameterization of Monovalent Ions Employing the Nonbonded Model. *J. Chem. Theory Comput.* **2015**, *11*, 1645−1657.
(59) Roe, D. R.; Cheatham, T. E., Iii PTRAJ and CPPTRAJ: Software for Processing and Analysis of Molecular Dynamics Trajectory Data. *J. Chem. Theory Comput.* **2013**, *9*, 3084−3095.
(60) Michaud-Agrawal, N.; Denning, E. J.; Woolf, T. B.; Beckstein, O. MDAnalysis: A toolkit for the analysis of molecular dynamics simulations. *J. Comput. Chem.* **2011**, *32*, 2319−2327.
(61) Peerless, J. S.; Bowers, G. H.; Kwansa, A. L.; Yingling, Y. G. Effect of C60 adducts on the dynamic structure of aromatic solvation shells. *Chem. Phys. Lett.* **2017**, *678*, 79−84.
(62) Peerless, J. S.; Bowers, G. H.; Kwansa, A. L.; Yingling, Y. G. Fullerenes in Aromatic Solvents: Correlation between Solvation-Shell Structure, Solvate Formation, and Solubility. *The Journal of Physical Chemistry B* **2015**, *119*, 15344−15352.
(63) Humphrey, W.; Dalke, A.; Schulten, K. VMD: Visual molecular dynamics. *Journal of Molecular Graphics* **1996**, *14*, 33−38.
(64) Bankura, A.; Carnevale, V.; Klein, M. L. Hydration structure of salt solutions fromab initiomolecular dynamics. *J. Chem. Phys.* **2013**, *138*, 014501.
(65) Gennes, P. G. d.; Alben, R.*The Physics of Liquid Crystals*; Oxford University Press: New York, 1993.
(66) Urban, S.; Gestblom, B.; Kuczyński, W.; Pawlus, S.; Würflinger, A. Nematic order parameter as determined from dielectric relaxation data and other methods. *Phys. Chem. Chem. Phys.* **2003**, *5*, 924−928.
(67) Barbosa, G. D.; Dach, E.; Liu, X.; Yip, N. Y.; Turner, C. H. Computational and experimental study of different brines in temperature swing solvent extraction desalination with amine solvents. *Desalination* **2022**, *537*, 115863.
(68) Guo, J.; Luo, S.; Liu, Z.; Luo, T. Direct Arsenic Removal from Water Using Non-Membrane, Low-Temperature Directional Solvent Extraction. *Journal of Chemical & Engineering Data* **2020**, *65*, 2938−2946.

https://doi.org/10.1021/acsestwater.2c00473
ACS EST Water 2023, 3, 400−409